

Figure S1 A subset of European *S. paradoxus* strains flocculate in a variety of conditions. Each photograph shows a liquid culture of a homozygous European *S. paradoxus* strain after overnight growth, with each row showing one strain and each column showing one treatment condition. Galactose, melibiose, and trehalose indicate media with the respective sugar as the sole carbon source. Ammonium sulfate indicates synthetic complete medium with 2% glucose and ammonium sulfate as the sole nitrogen source. The top two rows show representative flocculent strains and the bottom row shows the non-flocculent strain Z1.

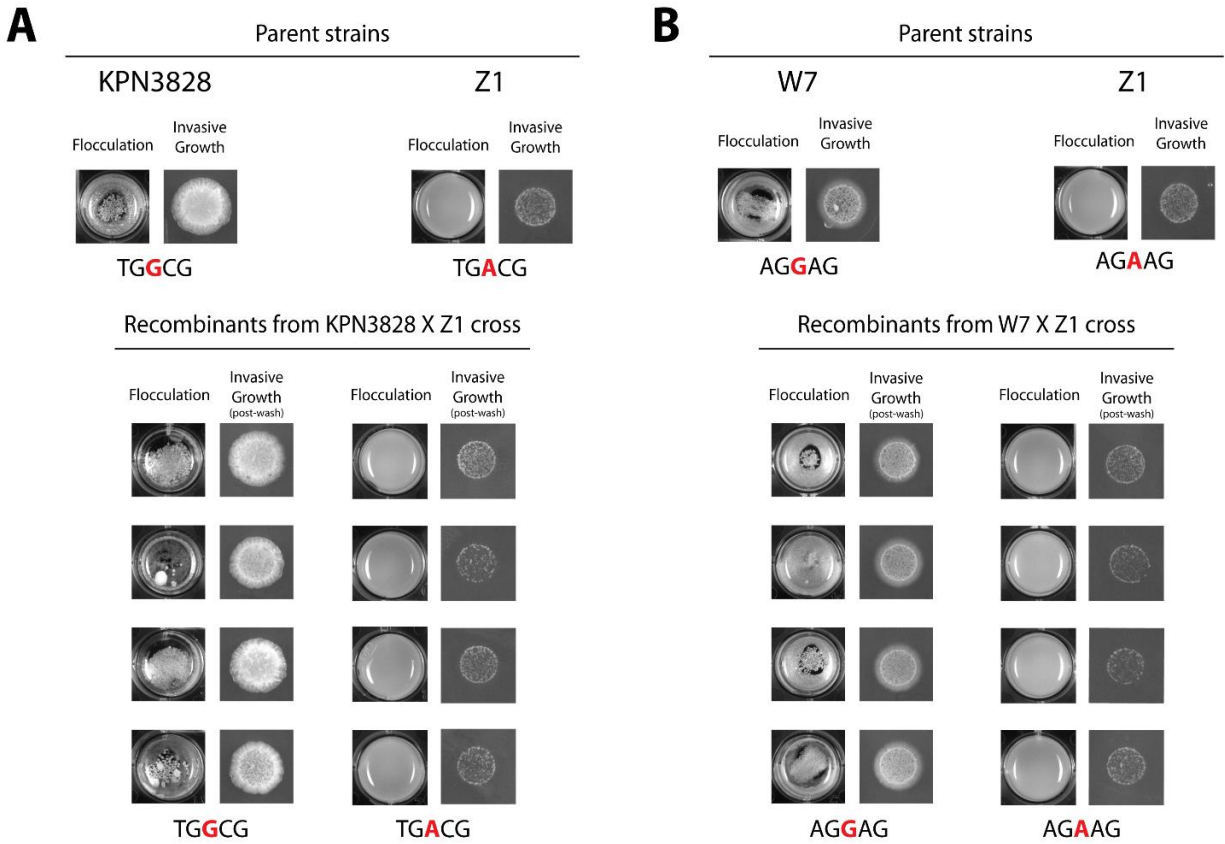
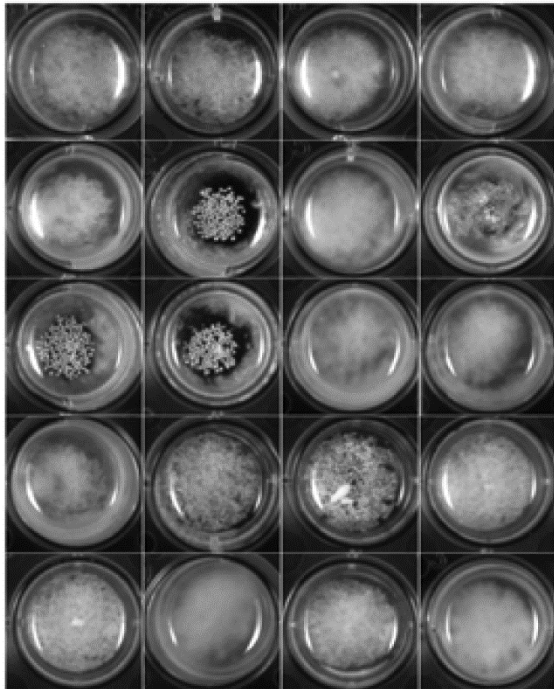
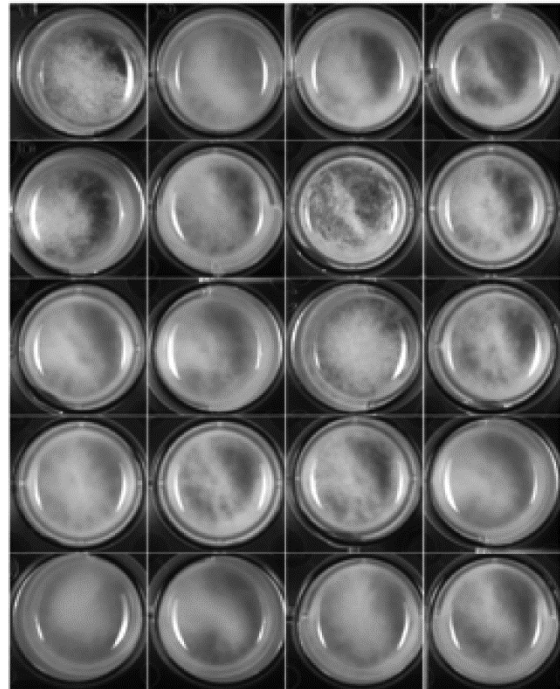


Figure S2 Flocculation and invasive growth are Mendelian traits linked to genetic variation at *IRA1* or *IRA2*. Each panel shows the results of linkage analysis of morphological traits and inheritance at an *IRA* gene, in a cross between a flocculent, invasive European strain and the non-flocculent, non-invasive European strain Z1. Each pair of photographs shows flocculation and invasive growth in one strain, assayed as in Figure 1 of main text. In each panel, the top row shows homozygote European strains used as parents in the respective cross, and each pair of photographs at the bottom shows one recombinant segregant from the cross, with segregants inheriting the variant allele of the *IRA* gene at left, and segregants inheriting the Z1 allele of the *IRA* gene at right. (A) The flocculent, invasive European homozygote KPN3828 crossed to Z1. Black and red text indicates genotype at positions 4437-4441 of *IRA2*. (B) The flocculent, invasive European homozygote W7 crossed to Z1. Black and red text indicates genotype at positions 5015-5019 of *IRA1*. In both (A) and (B), linkage between inheritance at the *IRA* gene and flocculation is significant at $p = 0.0007$.

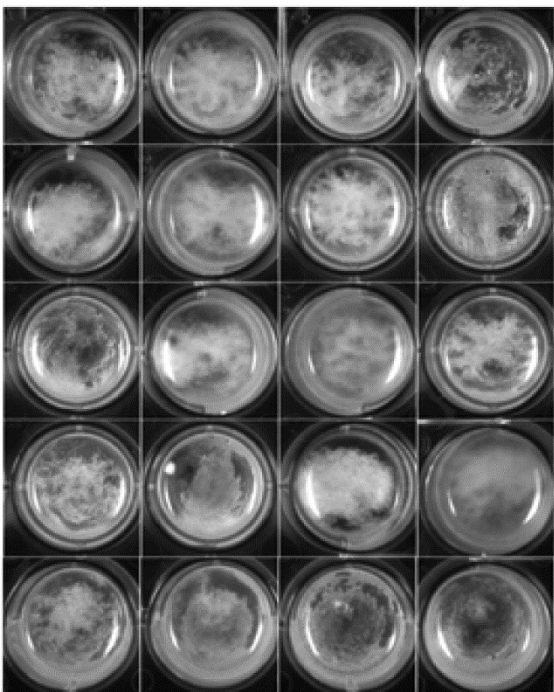
CBS5829 X KPN3828 recombinants



W7 X Q31.4 recombinants



W7 X KPN3829 recombinants



W7 X KPN3828 recombinants



Figure S3 Two distinct loci underlie flocculation across strains. Each panel shows liquid cultures of recombinant progeny from one complementation cross between two European flocculent parent strains. Each row shows cultures of YPD medium inoculated from each of the four spores of one tetrad and grown overnight as in Figure 1A of the main text. All progeny from each cross exhibit flocculation except the cross of W7 with KPN3828 (lower right), indicating that distinct loci underlie the flocculation trait in the latter and for each other pair of European parent strains tested, the two strains share the same causal locus.

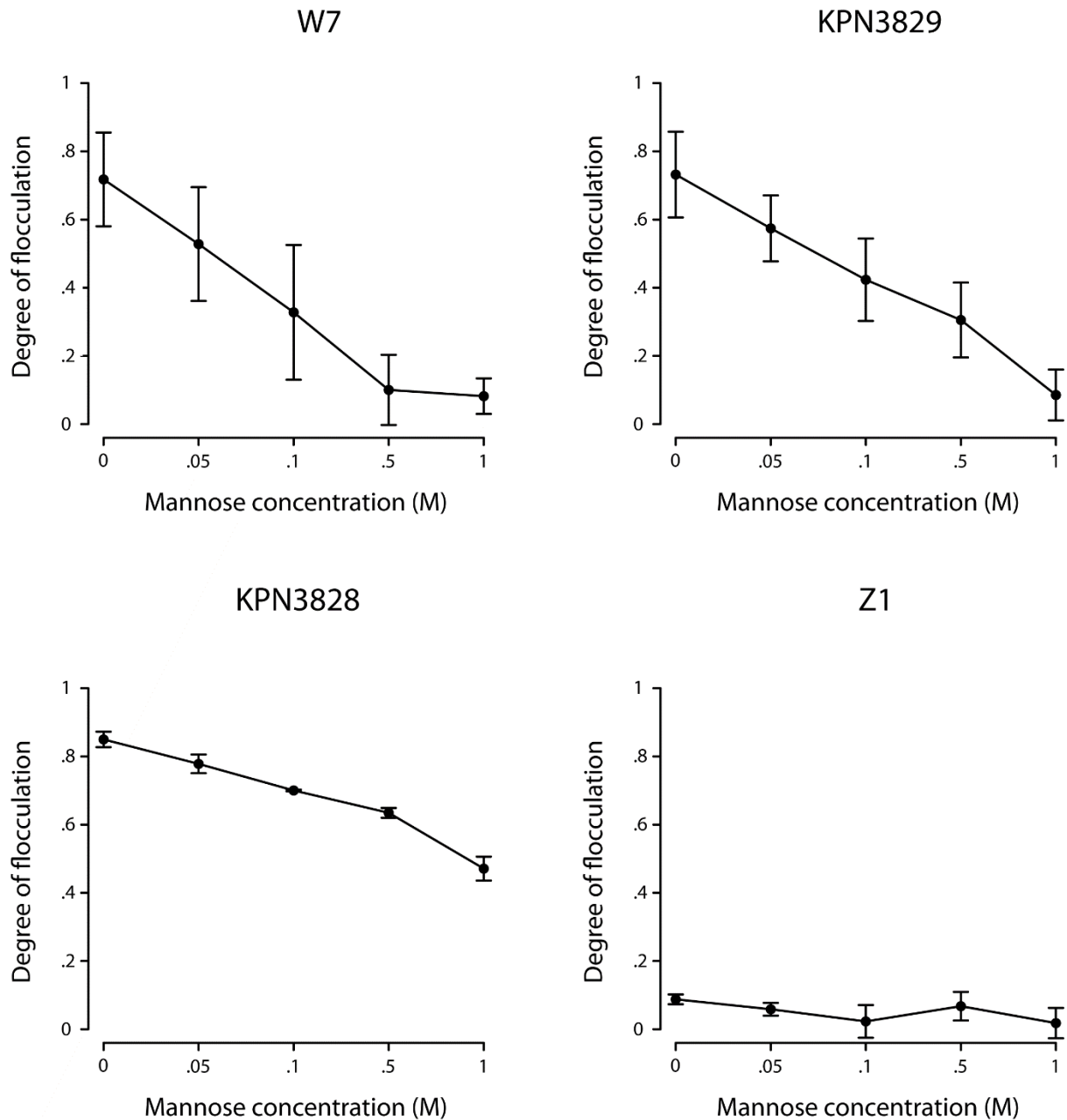


Figure S4 Flocculation is inhibited by mannose. Each panel shows the response of flocculation to increasing concentrations of mannose in one European *S. paradoxus* strain. In each panel, the x axis reports mannose concentration and the y axis reports flocculation, as measured by cell density at the top of a liquid culture allowed to settle, normalized by the analogous quantity from a culture treated with EDTA. Each data point represents the mean of three replicate cultures, and error bars report one standard deviation. Note that mannose had no effect on spatial inhomogeneity of cultures of the non-flocculent European strain Z1 (lower right), while the other three flocculent strains (see Figure 1A of the main text), are sensitive to mannose.

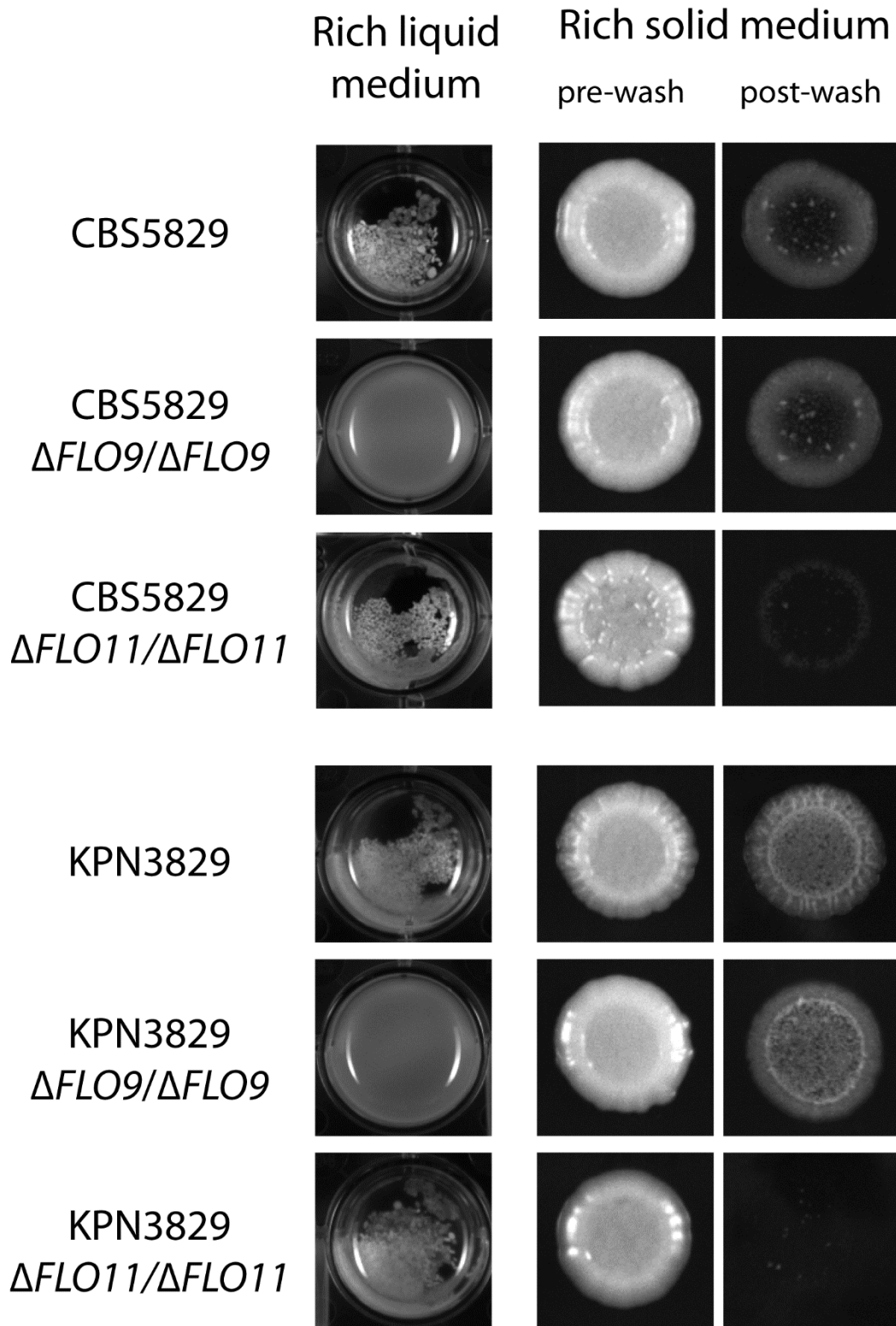


Figure S5 *FLO9* and *FLO11* are terminal effectors of flocculation and invasive growth in multiple *S. paradoxus* strains. Data are as in Figure 2 of the main text except that flocculent European strains CBS5829 and KPN3829 were analyzed.

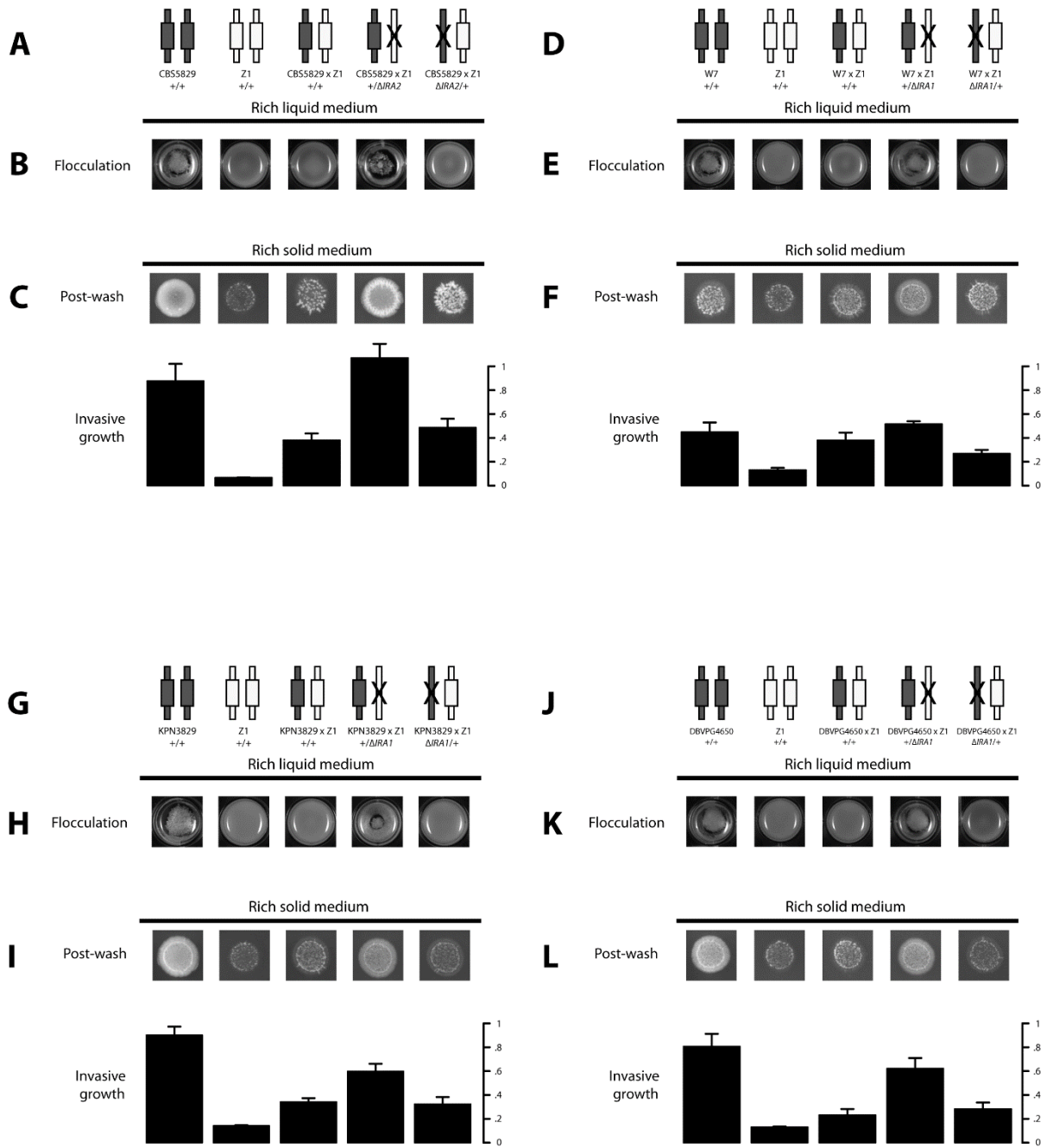


Figure S6 Variation at *IRA1* and *IRA2* underlie flocculation and invasive growth. Data are as in Figure 3 of the main text, except that flocculent European strains CBS5829 (A-C), W7 (D-F), KPN3829 (G-I), and DVBPG4650 (J-L) were analyzed.

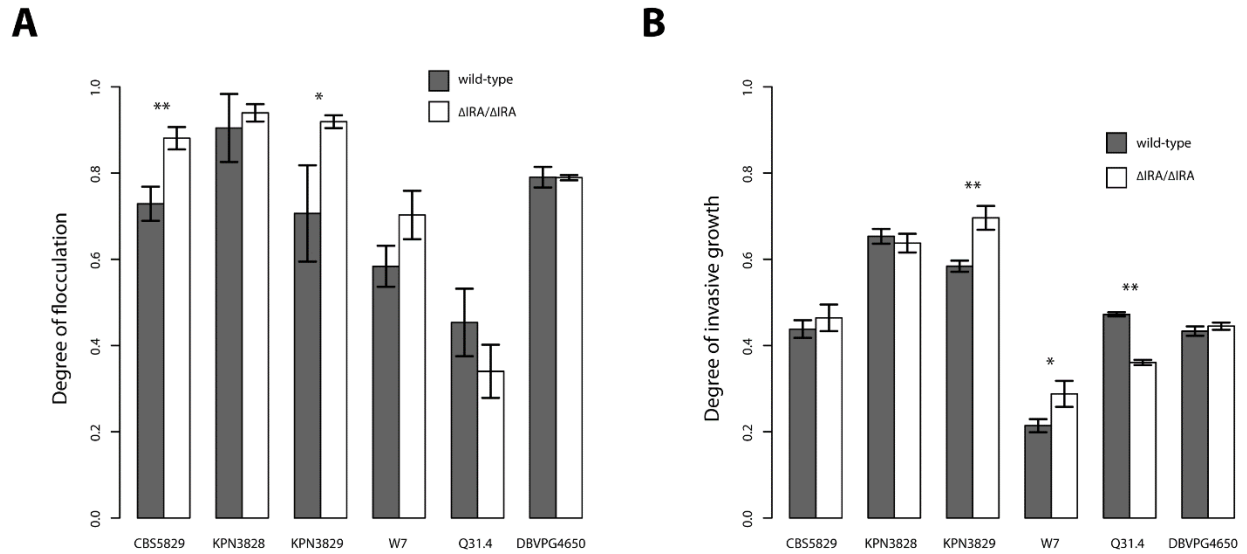


Figure S7 Variant *IRA1* and *IRA2* alleles act as partial or complete losses of function. Each panel reports measurements of one morphology in European *S. paradoxus* strains and their derivatives harboring engineered mutations in either *IRA1* or *IRA2*. In a given panel, each pair of bars reports data for two strains: a European strain and its derivative bearing an engineered mutation at the *IRA* gene found to underlie its morphologies (see Figure 3 and Figure S6). (A) Flocculation, measured as in Supplementary Figure 4. (B) Invasive growth, measured as in Figure 1B of the main text. Quantitative differences between wild type and *IRA* deletion strain phenotypes in both panels were assessed by Welch's *t* test (*, $p < 0.05$, **, $p < 0.001$). Δ , engineered loss-of-function allele.

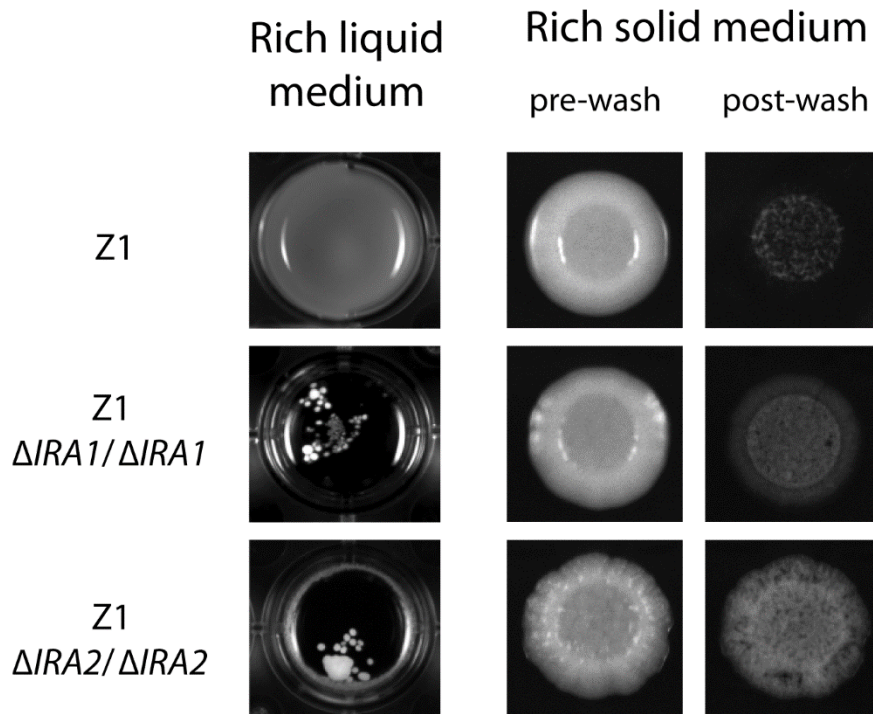


Figure S8 Engineered mutation of either *IRA1* or *IRA2* is sufficient for flocculation and invasive growth. Each row reports morphologies of one homozygous derivative of the non-flocculent, non-invasive European strain Z1. Left photographs show overnight cultures in rich liquid medium, and right photographs show the results of invasive growth assays of colonies grown on rich solid medium, both as in Figure 1 of the main text. Δ , engineered loss-of-function allele.

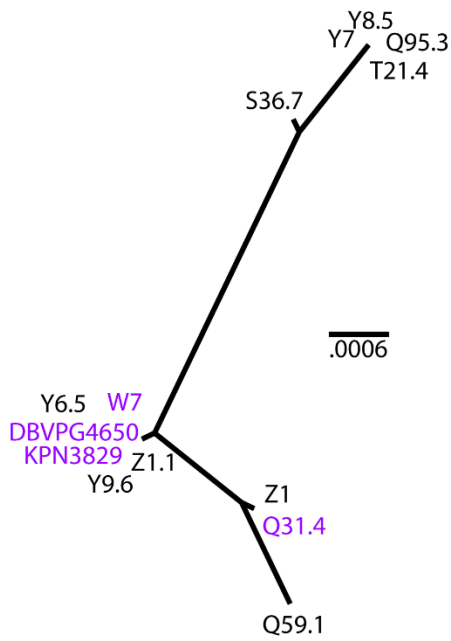
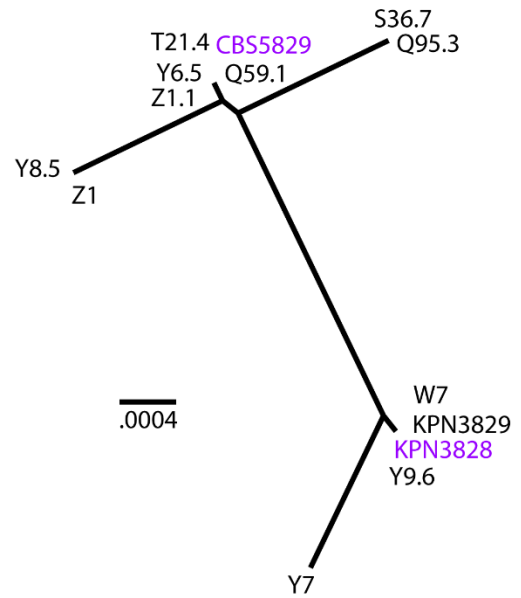
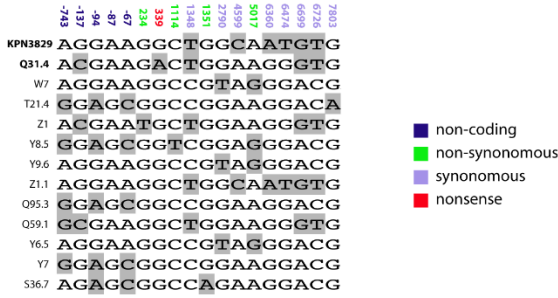
A**B**

Figure S9 Phylogeny of promoter regions of *IRA1* and *IRA2*. Maximum likelihood phylogeny inferred from 800bp of nucleotide sequence upstream of the *IRA1* (A) or *IRA2* (B) coding region. Identifiers of strains in which *IRA1* or *IRA2* underlie flocculent and invasive growth traits are colored purple. Scale bars indicate frequencies of base pair substitutions per site.

A



B

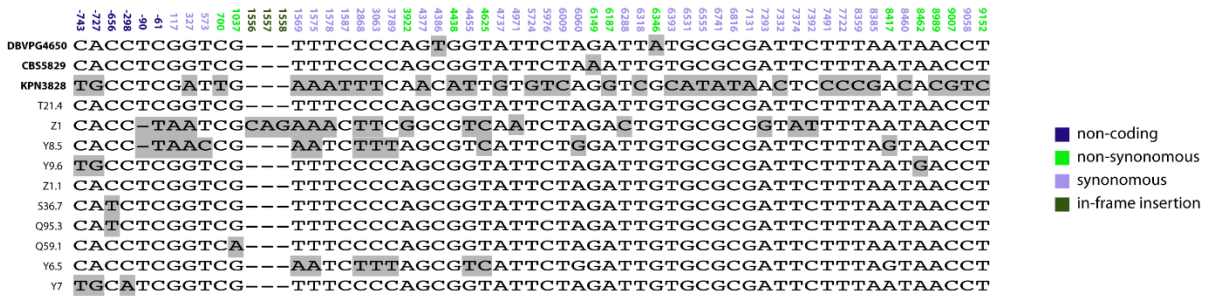


Figure S10 *IRA1* and *IRA2* genes from flocculent/invasive strains do not share derived polymorphisms. Shown are polymorphic sites in the *IRA1* (A) or *IRA2* (B) coding sequence and 800bp of promoter region for the indicated *S. paradoxus* strains. Minor alleles at each site in the alignment are highlighted in grey. Positions of each site relative to the start of the coding sequence are indicated above the alignment and color-coded to indicate the effect of each minor allele on the protein sequence. Original isolates of the five flocculent/invasive strains were used for sequencing, with names indicated in bold.

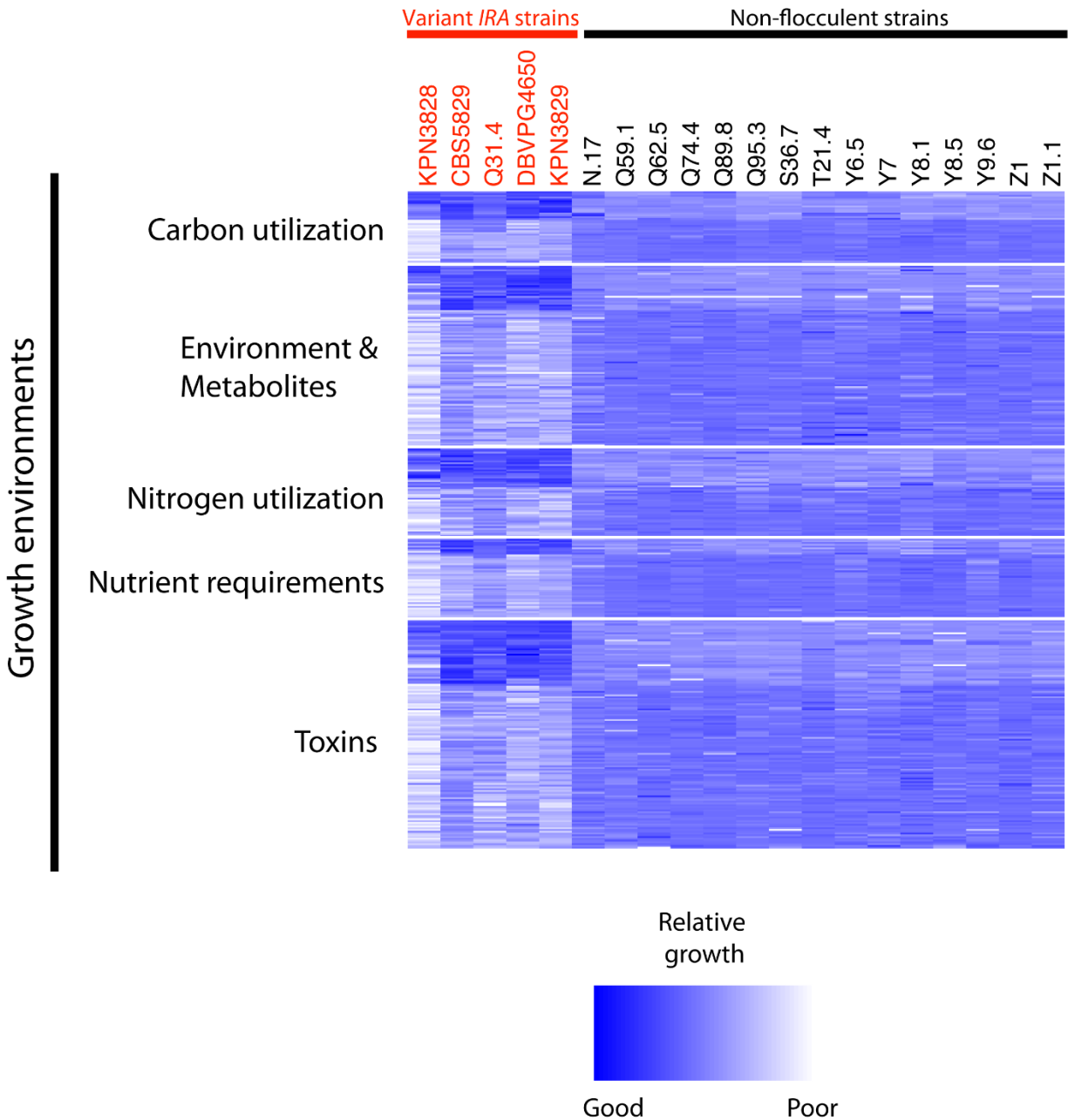
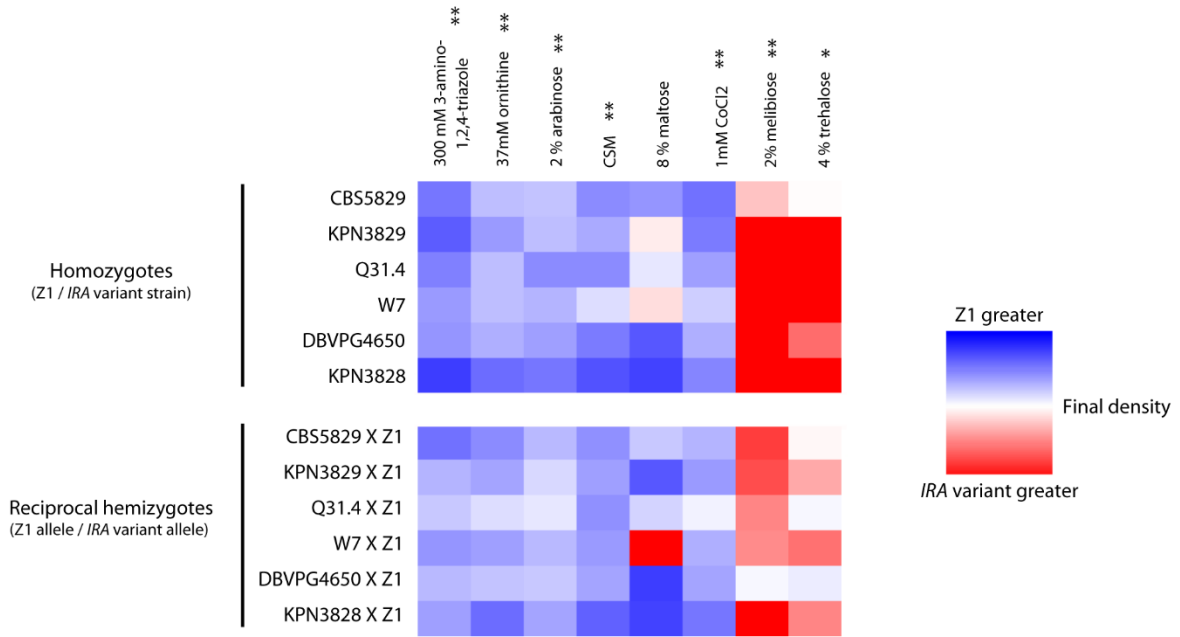


Figure S11 Hundreds of growth traits across environmental treatments associate with variants in *IRA1* and *IRA2*. Each column reports fitness measurements from a liquid culture of one strain, and each row reports measurements in one condition. For each row, measurements of lag time before resumption of log-phase growth after dilution into fresh medium, growth rate in log phase, or final culture density in stationary phase were taken from (Warringer et al. 2011) and normalized against the median across strains. Shown is each environment-parameter combination for which the difference between flocculent and invasive strains bearing variants in *IRA1* or *IRA2*, and the remainder of strains in the data set, reached a significance level corresponding to a false discovery rate less than 5%. Raw measurements for all environment-parameter combinations and significance estimates are provided in File S1.

A



B

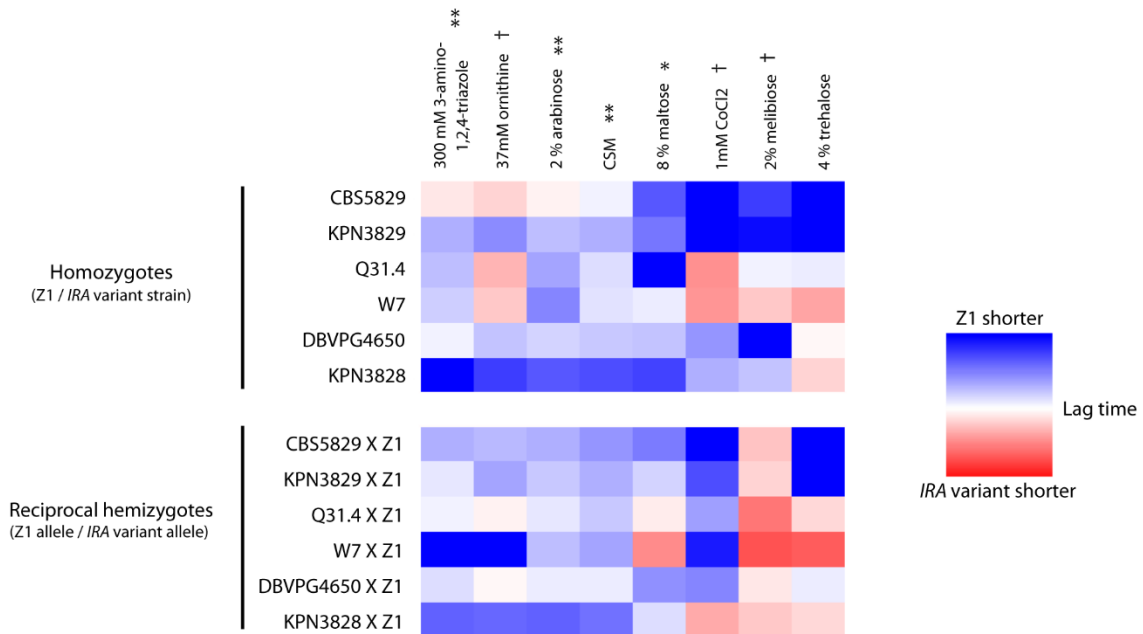


Figure S12 Variation at *IRA1* and *IRA2* underlies differences between strains in final culture density and lag in multiple conditions. Data are as in Figure 5B of the main text, except that final culture density in stationary phase (A) or lag time before resumption of log-phase growth after dilution into fresh medium (B) were analyzed. Media marked by † are those in which hemizygote hybrid strains bearing the variant *IRA* genes differed significantly from hemizygote hybrid strains bearing the Z1 allele at the *IRA* genes (Wilcoxon rank-sum test, $p < 0.05$ after Bonferroni correction), but homozygote European strains bearing variant *IRA* genes did not differ significantly from Z1.

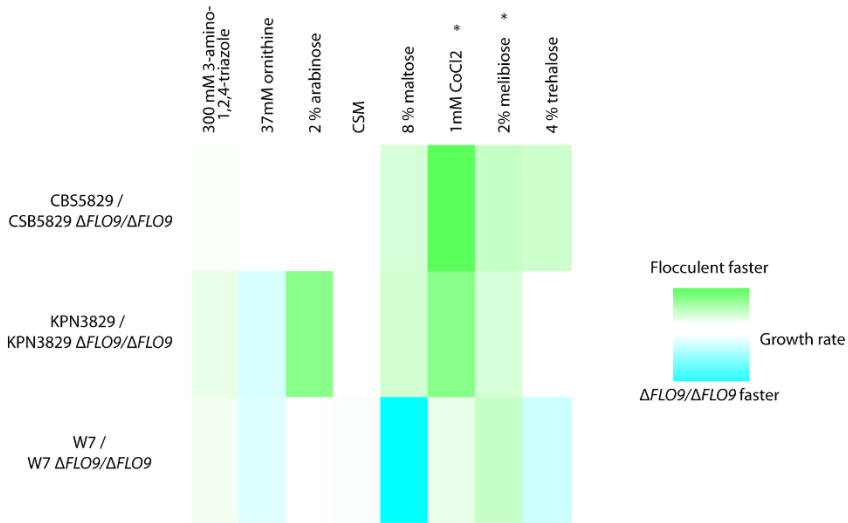
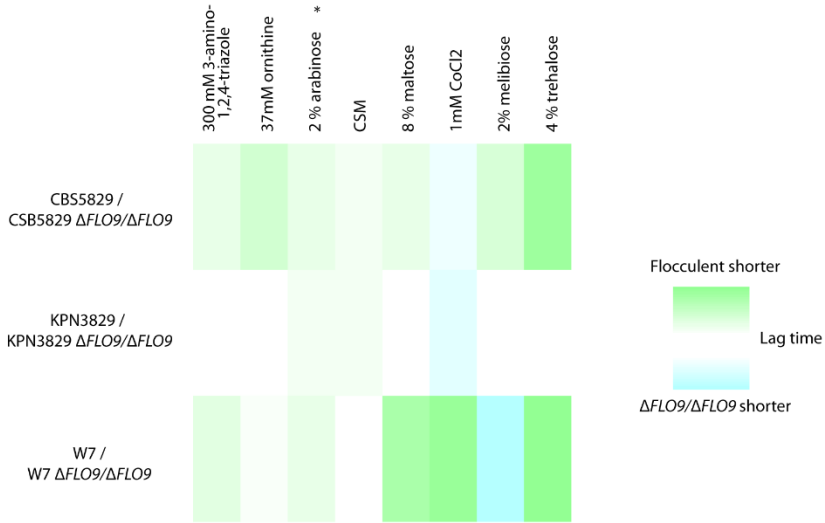
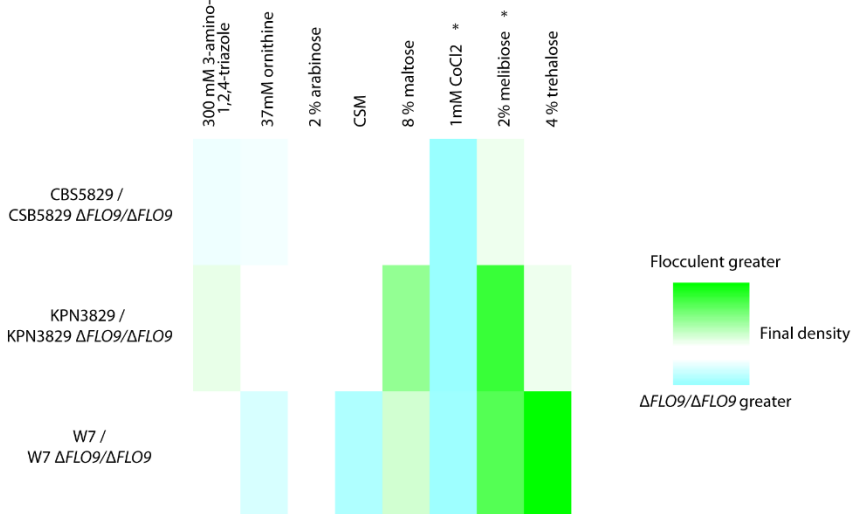
A**B****C**

Figure S13 Effect of flocculation on culture growth. Each panel reports one growth parameter measured in liquid cultures of homozygous flocculent European strains and their engineered non-flocculent derivatives. In a given panel, each row reports results from one European strain and each row reports measurements in one medium. Color in each cell reports the indicated growth parameter in the indicated condition as a ratio of measurements from two strains: the indicated flocculent European strain and an isogenic non-flocculent strain homozygous for a null allele of *FLO9*. (A) Growth rate; (B) lag time; (C) cell density in stationary phase. In a given panel, media marked by * are those in which growth of flocculent European strains differed significantly from non-flocculent *FLO9* mutants (Wilcoxon rank-sum test, $p < 0.05$ after Bonferroni correction). Δ , engineered loss-of-function allele. Raw measurements and significance estimates are given in Supplementary File S3.

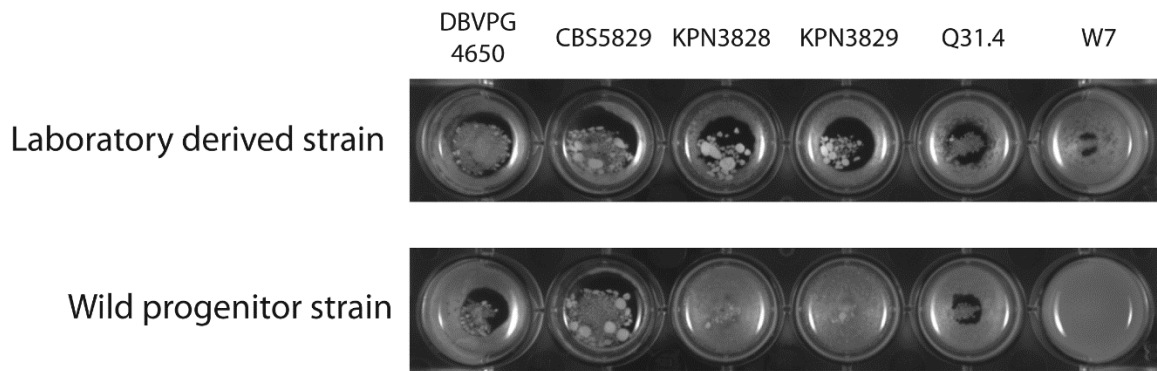
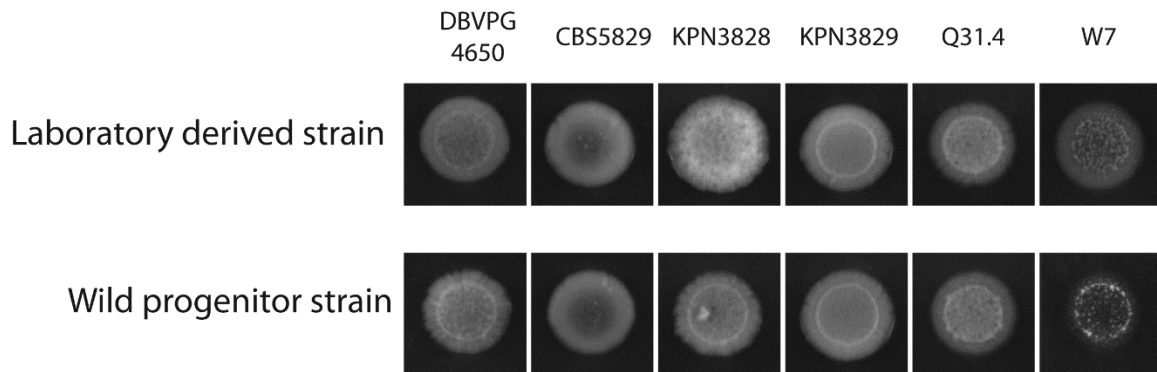
A**B**

Figure S14 Most wild European *S. paradoxus* strains exhibit the same morphologies as their laboratory derivatives. Each panel shows morphologies in wild European *S. paradoxus* strains (top row) and their monosporic laboratory derivatives (bottom row). (A) Photographs of cultures after overnight growth in liquid rich medium as in Figure 1A of the main text. (B) Results of invasive growth assays of colonies grown on solid medium as in Figure 1B of the main text.

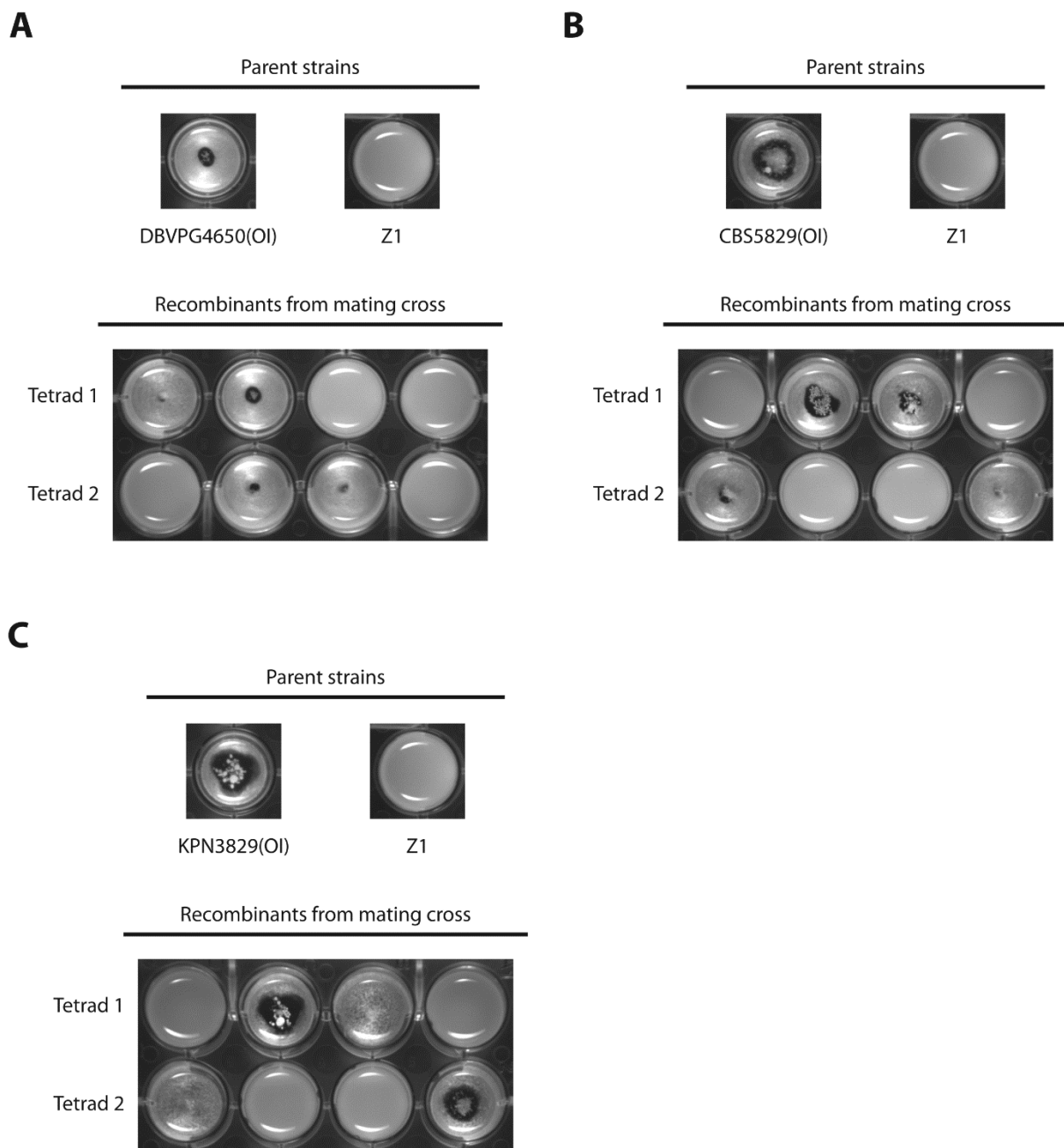


Figure S15 Flocculation is a Mendelian trait in wild progenitor strains. Each panel shows the growth phenotype in rich liquid media of a wild progenitor strain (original isolate, OI) and the Z1 non-flocculent strain (top), and recombinant progeny from a mating between these two parental strains (bottom). Recombinant progeny represent all four spores from two tetrad dissections, as indicated. (A) The flocculent wild progenitor of the DBVPG4650 strain crossed to Z1. (B) The flocculent wild progenitor of the CBS5829 strain crossed to Z1. (C) The flocculent wild progenitor of the KPN3829 strain crossed to Z1.

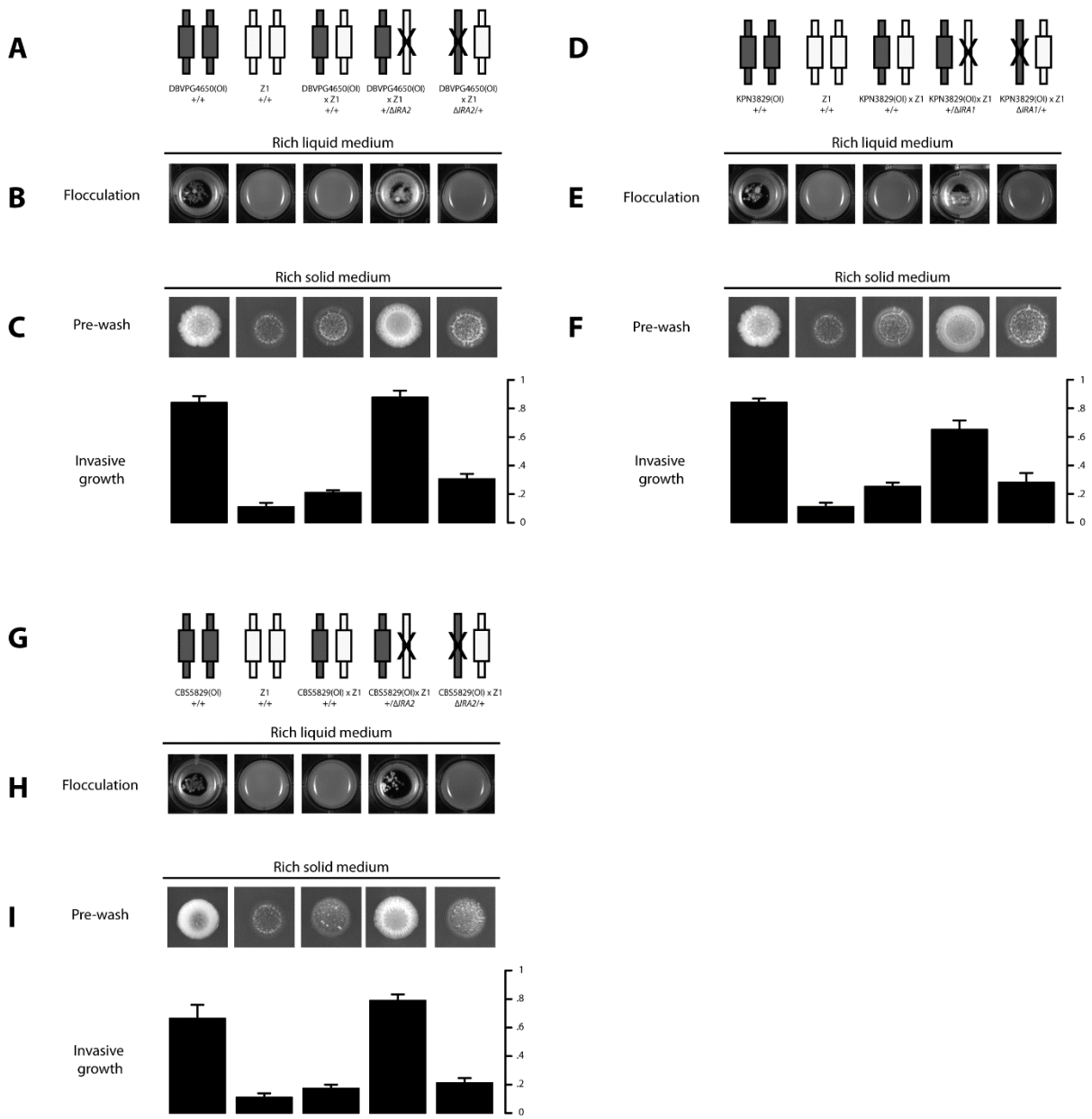


Figure S16 Variation at *IRA1* and *IRA2* underlie flocculation and invasive growth in wild progenitor strains. Data are as in Figure 3 of the main text and Figure S6, except that the wild progenitors (original isolates, OI) of strains DBVPG4650 (A-C), KPN3829 (D-F) and CBS5829 (G-I), were analyzed.

Files S1-S3

Available for download at <http://www.genetics.org/lookup/suppl/doi:10.1534/genetics.113.155341/-/DC1>

File S1 Association test of *IRA* gene variants with growth parameters across European *S. paradoxus*. Each row reports the results of a Wilcoxon rank-sum test comparing the indicated growth measurement from (Warringer et al. 2011) between two sets of European *S. paradoxus* strains: those without the flocculation and invasive growth morphologies (Z1, Y7,N-17, T21.4, Y6.5, Q59.1, Q62.5, Q89.8, Q95.3, S36.7, Z1.1, Y9.6, Q74.4, Y8.5, Y8.1, and Q69.8), and those whose morphologies were the result of variation at *IRA1* or *IRA2* (KPN3828, KPN3829, CBS5829, DBVPG4650, and Q31.4).

File S2 Growth measurements in wild-type European *S. paradoxus* homozygotes and engineered *IRA* gene reciprocal hemizygotes. Each tab gives analysis of one growth parameter. In a given tab, the first 21 rows report measurements of the indicated parameter in the indicated condition, in a strain falling into one of two classes: European homozygote diploid strains, and reciprocal hemizygote hybrid diploids bearing an engineered loss-of-function mutation in one of the two homologs of an *IRA* gene (see Figure 3A of the main text for schematic). All growth values reported are the mean of three replicate cultures, except for values reported for the Z1 strain which are the mean of two replicate cultures. The last two rows report comparisons of sets of strains defined based on genotype at the *IRA* genes. Significance, parents: nominal *p* value from Wilcoxon rank-sum test comparing fitness differences between the complete set of flocculent European strains (three replicate cultures per strain) and the non-flocculent European strain Z1 (six total replicate cultures). Significance, reciprocal hemizygotes: nominal *p* value from Wilcoxon rank-sum test for significant fitness differences between the complete set of hemizygotes bearing the Z1 allele at the respective *IRA* gene (three replicate cultures per strain), and the complete set of hybrid hemizygotes bearing the allele at the respective *IRA* gene associated with flocculation and invasive growth (three replicate cultures per strain).

File S3 Growth measurements in European homozygote strains and their *FLO9*-null non-flocculent derivatives. Each tab gives analysis of one growth parameter. In a given tab, the first six rows report measurements of the indicated parameter in the indicated growth condition, in a flocculent European homozygote or its non-flocculent derivative homozygous for an engineered loss-of-function allele at *FLO9*. Δ , engineered loss-of-function allele. All growth values reported are the mean of three replicate cultures. Significance, nominal *p* value from Wilcoxon rank-sum test comparing fitness between European homozygotes (three replicate cultures per strain) and *FLO9* nulls (three replicate cultures per strain).

Table S1 Strains used in this work

Strain	Parent(s)	Genotype	Source
Q31.4			NCYC
Q32.3			NCYC
Q59.1			NCYC
Q62.5			NCYC
Q69.8			NCYC
Q74.4			NCYC
Q89.8			NCYC
Q95.3			NCYC
S36.7			NCYC
T21.4			NCYC
W7			NCYC
Y6.5			NCYC
Y7			NCYC
Y8.1			NCYC
Y8.5			NCYC
Y9.6			NCYC
Z1			NCYC
Z1.1			NCYC
N-17			NCYC
CBS432			NCYC
CBS5829			NCYC
DBVPG4650			NCYC
KPN3828			NCYC
KPN3829			NCYC
YJR66	Q31.4 X Z1		this work
YJR44	W7 X Z1		this work
YJR119	CBS432 X Z1		this work
YJR78	CBS5829 X Z1		this work
YJR45	KPN3828 X Z1		this work
YJR39	KPN3829 X Z1		this work
YJR65	DBVPG4650 X Z1		this work
YJR46	W7 X KPN828		this work
YJR129	KPN3829 X W7		this work
YJR130	CBS5829 X KPN3828		this work
YJR91	W7	$\Delta FLO9::kanMX/\Delta FLO9::kanMX$	this work
YJR123	KPN3829	$\Delta FLO9::kanMX/\Delta FLO9::kanMX$	this work
YJR125	CBS5829	$\Delta FLO9::kanMX/\Delta FLO9::kanMX$	this work
YJR60	W7	$\Delta FLO11::kanMX/\Delta FLO11::kanMX$	this work
YJR59	KPN3829	$\Delta FLO11::kanMX/\Delta FLO11::kanMX$	this work
YJR127	CBS5829	$\Delta FLO11::kanMX/\Delta FLO11::kanMX$	this work
YJR67	W7	$\Delta flo1::kanMX/\Delta flo1::kanMX$	this work
YJR68	W7	$\Delta flo5::kanMX/\Delta flo5::kanMX$	this work
YJR69	W7	$\Delta flo10::kanMX/\Delta flo10::kanMX$	this work
YJR97	YJR66	$\Delta IRA1::kanMX/IRA1$ (Q31.4)	this work
YJR98	YJR66	$\Delta IRA1::kanMX/IRA1$ (Z1)	this work
YJR58	YJR44	$\Delta IRA1::kanMX/IRA1$ (W7)	this work
YJR57	YJR44	$\Delta IRA1::kanMX/IRA1$ (Z1)	this work
YJR120	YJR39	$\Delta IRA1::kanMX/IRA1$ (KPN3829)	this work
YJR121	YJR39	$\Delta IRA1::kanMX/IRA1$ (Z1)	this work
YJR117	YJR65	$\Delta IRA1::kanMX/IRA1$ (DBVPG4650)	this work
YJR118	YJR65	$\Delta IRA1::kanMX/IRA1$ (Z1)	this work
YJR105	YJR78	$\Delta IRA2::kanMX/IRA2$ (CBS5829)	this work
YJR106	YJR78	$\Delta IRA2::kanMX/IRA2$ (Z1)	this work
YJR134	YJR45	$\Delta IRA2::kanMX/IRA2$ (KPN3828)	this work

YJR135	YJR45	<i>ΔIRA2::kanMX/IRA2</i> (Z1)	this work
YJR100	Z1	<i>ΔIRA2::kanMX/ΔIRA2::kanMX</i>	this work
YJR101	Z1	<i>ΔIRA1::kanMX/ΔIRA1::kanMX</i>	this work
Q31.4(OI)			V. Koufopanou
W7(OI)			V. Koufopanou
KPN3828(OI)			G. Liti
CBS5829(OI)			G. Liti
DBVPG4650(OI)			G. Liti
KPN3829(OI)			G. Liti

OI, Original isolate.

Table S2 *IRA1* and *IRA2* have high nucleotide diversity in *S. paradoxus* populations

Population ^a	Proportion CDS with $\pi > IRA1^b$	Proportion CDS with $\pi > IRA2^c$
European	.307	.004
American	.049	.071
Far East	.052	.037

^a *S. paradoxus* population as in (Liti et al. 2009).

^b The proportion of gene-coding regions (CDS) with higher nucleotide diversity (π) than *IRA1* across the indicated population.

^c The proportion of gene-coding regions with higher nucleotide diversity than *IRA2* across the indicated population.